

See discussions, stats, and author profiles for this publication at: <https://www.researchgate.net/publication/24216968>

# Spectroscopic, structural and theoretical studies of novel, potentially cytotoxic 4-acridonecarboxamide imines

ARTICLE *in* SPECTROCHIMICA ACTA PART A MOLECULAR AND BIOMOLECULAR SPECTROSCOPY · MARCH 2009

Impact Factor: 2.35 · DOI: 10.1016/j.saa.2009.02.016 · Source: PubMed

CITATIONS

6

READS

47

## 11 AUTHORS, INCLUDING:



**Ivan Danihel**

Pavol Jozef Šafárik University in Košice

33 PUBLICATIONS 148 CITATIONS

SEE PROFILE



**Pavol Kristian**

Pavol Jozef Šafárik University in Košice

106 PUBLICATIONS 667 CITATIONS

SEE PROFILE



**Danica Sabolova**

Pavol Jozef Šafárik University in Košice

24 PUBLICATIONS 216 CITATIONS

SEE PROFILE



**Maria Kozurkova**

Pavol Jozef Šafárik University in Košice

50 PUBLICATIONS 268 CITATIONS

SEE PROFILE



## Spectroscopic, structural and theoretical studies of novel, potentially cytotoxic 4-acridonecarboxamide imines

Zdenka Fröhlichová<sup>a</sup>, Ján Imrich<sup>a,\*</sup>, Ivan Danihel<sup>a</sup>, Pavol Kristian<sup>a</sup>, Stanislav Böhm<sup>b</sup>, Danica Sabolová<sup>a</sup>, Mária Kožurková<sup>a</sup>, Ol'ga Hritzová<sup>a</sup>, Branislav Horváth<sup>c</sup>, Tatiana Bušová<sup>a</sup>, Karel D. Klika<sup>d</sup>

<sup>a</sup> Institute of Chemistry, Faculty of Science, P.J. Šafárik University, SK-041 67 Košice, Slovak Republic

<sup>b</sup> Department of Organic Chemistry, Institute of Chemical Technology, CZ-166 28 Prague, Czech Republic

<sup>c</sup> Institute of Chemistry, Faculty of Natural Sciences, Comenius University, SK-842 15 Bratislava, Slovak Republic

<sup>d</sup> Department of Chemistry, University of Turku, FIN-20014 Turku, Finland

### ARTICLE INFO

#### Article history:

Received 6 October 2008

Received in revised form 5 February 2009

Accepted 6 February 2009

#### Keywords:

Azomethines

Ketimines

Acridonecarboxyhydrazides

NMR spectroscopy

Quantum chemical calculations

### ABSTRACT

Ten novel, potentially intercalating 4-acridonecarboxamide azomethines and ketimines have been prepared by the condensation reaction of 9-oxo-9,10-dihydroacridine-4-carboxylic acid hydrazide with various aldehydes and ketones. The structures of the compounds were characterized spectroscopically by NMR (<sup>1</sup>H, <sup>13</sup>C, <sup>15</sup>N nuclei and 2D experiments), UV–vis, IR and fluorescence methods and by quantum chemical calculations using DFT at the B3LYP/6-311+G(d,p) level of theory and semiempirical ZINDO and AM1 methods. NMR chemical shift variations for C-4' were assessed due to changes in the polarizability of the imine C<sub>4</sub>=N<sub>3</sub> bond rather than direct inductive effects arising from the C-4' substituents. In concert with this was the reversed order observed for the N-3' chemical shifts with DFT-calculated atomic charges confirming the bond polarization. Both intra- and intermolecular hydrogen bonds between the acridone NH hydrogen and the amidic carbonyl oxygen were found to exist by FT-IR spectroscopy. Quantum chemical calculations were used to evaluate the configurational, tautomeric, conformational and hydrogen bonding states of the molecules as well as predict the NMR and IR data. The hypsochromic shifts observed in the UV–vis spectra upon changing from *m*-cresol to DMA, DMF or methanol were evaluated in terms of solvent polarity (giving rise to solvated excited state destabilization) and solvent aromaticity (giving rise to solvated excited state stabilization). The fluorescence of the compounds was modest, except for the 2,6-dichloro derivative, with respect to 9-isothiocyanatoacridine.

© 2009 Elsevier B.V. All rights reserved.

## 1. Introduction

The convoluted IR spectra arising from two carbonyl and two N–H groups and their attendant spectroscopic and structural interactions, the structural diversity arising from an imine N=C double bond and an amide bond as well as the capabilities for both intra- and intermolecular hydrogen bonding are among the attributes rendering the azomethines and ketimines studied herein (Fig. 1) spectroscopically interesting systems. Also, imines derived from 9-oxo-9,10-dihydroacridine-4-carboxylic acid hydrazide have use in organic synthesis for the production of biologically interesting heterocycles, e.g. acridoneoxadiazoles [1].

Substituted 9-acridones [2], as well as azomethines and ketimines [3], have been studied recently both experimentally and theoretically. In the comparative study [3] of azomethines and ketimines, it was found that the prepared azomethines occurred

only as one geometric isomer whilst two geometric isomers were formed during the preparation of the ketimines. Herein, we examine experimentally and theoretically 4-acridonecarboxamide imine molecular systems, compounds (1)–(10), which include examples of both classes. The state of intra- and intermolecular hydrogen bonding within these systems was also examined. Since a number of acridine derivatives are notable for their intercalating [4] and fluorescent properties [5] with many being utilized as sensitive biomarkers or as chemotherapeutic agents [6], attention was therefore also focused on the fluorescence properties of the compounds.

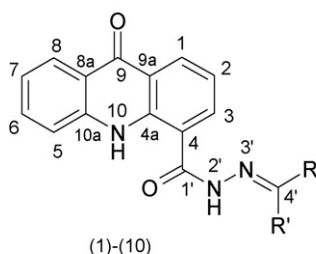
## 2. Experimental

### 2.1. Materials

All solvents were dried prior to use and the commercially acquired aldehydes and ketones were used without further purification. 9-Oxo-9,10-dihydroacridine-4-carboxylic acid hydrazide was prepared starting from 2,2'-iminodibenzoic acid

\* Corresponding author. Tel.: +421 55 2342334.

E-mail address: [jan.imrich@upjs.sk](mailto:jan.imrich@upjs.sk) (J. Imrich).



Cmpd	R	R'
(1)	phenyl	H
(2)	2-chlorophenyl	H
(3)	4-methoxyphenyl	H
(4)	4-bromophenyl	H
(5)	2,6-dichlorophenyl	H
(6)	2,4,6-trimethylphenyl	H
(7)	methyl	H
(8)	<i>tert</i> -butyl	H
(9)	phenyl	methyl
(10)	methyl	methyl

Fig. 1. The synthesized compounds under study.

according to literature procedures [1,7]. The reference compounds 9-isothiocyanatoacridine, acridone, 4-methyl acridone, 4-acridone carboxylic acid, benzoic acid (1-phenyl-methylidene) hydrazide and benzoic acid (1-phenyl-ethylidene) hydrazide were also synthesized [8,9].

## 2.2. Characterization techniques

1D and 2D NMR spectra were measured on a Varian Mercury Plus NMR spectrometer operating at 400 MHz for  $^1\text{H}$  and 100 MHz for  $^{13}\text{C}$ . Samples were run in  $\text{DMSO}-d_6$  using TMS as an internal reference at 298 K. In addition to 1D  $^1\text{H}$  and  $^{13}\text{C}$  spectra, a series of standard library experiments were also acquired: H,H-COSY, H,H-NOESY, gHSQC and gHMBC.  $^{15}\text{N}$  NMR chemical shifts were measured indirectly using  $^1\text{H}$ – $^{15}\text{N}$  correlation experiments on a Varian Inova NMR spectrometer operating at 599.78 for  $^1\text{H}$  and 60.78 MHz for  $^{15}\text{N}$  and equipped with a 5 mm triple resonance probe  $^1\text{H}\{^{13}\text{C},^{15}\text{N}\}$  possessing a z-gradient coil. The 90° pulse lengths were 6.8  $\mu\text{s}$  for  $^1\text{H}$  and 37.8  $\mu\text{s}$  for  $^{15}\text{N}$ . The gHSQCAD pulse sequence was used for one bond correlations and the gHMBCAD pulse sequence for multiple bond correlations. Both sequences were used as supplied with Chempack 4.1. HSQC spectra were acquired as  $2400 \times (200\text{--}320)$  data matrices with 4–16 transients per  $t_1$  increment, spectral windows were 8000 Hz ( $f_2$ ) and 14,000 Hz ( $f_1$ ) wide. The HMBC spectra were recorded with a spectral width of 8000 Hz in the  $^1\text{H}$  dimension consisting of 4096 points and a spectral width of 14,000 Hz consisting of 200–320 increments in the  $^{15}\text{N}$  dimension with 16–80 transients acquired per  $t_1$  increment. The multiple-bond delay was set to 166.7 ms. The data were linear predicted to twice the acquired increments in  $t_1$  and zero-filled to 2048 points. The unified chemical shift scale was used for  $^{15}\text{N}$  with nitromethane as a secondary standard ( $\delta = 0.0$  ppm;  $\Xi = 10.1367670$ ) [10].

IR spectra over the region  $4000\text{--}400\text{ cm}^{-1}$  were recorded at room temperature using FT-IR spectrometers: a Nicolet Avatar 330 for pellets of (1)–(10) in potassium bromide and a Nicolet 6700 FT-IR for derivatives (1) and (9) in  $\text{CS}_2$  solution. KBr and infrasil cuvettes of length 0.1, 1.04 and 10 mm were used.

UV–vis spectra were recorded on a Varian Cary 100 Bio spectrophotometer. Fluorescence measurements were performed using a Varian Cary Eclipse spectrofluorometer with a slit width of 10 nm for the excitation and emission beams in methanol. Fluorescence intensities are expressed in arbitrary units. Elemental analysis was performed using a PerkinElmer CHN 2400 analyzer.

## 2.3. Quantum chemical calculations

DFT quantum chemical calculations (geometry optimization, keyword = *opt*, and frequency calculations, keyword = *freq*) of compounds (1)–(10) were performed at the B3LYP/6-311+G(d,p) level of theory [11] using Gaussian03 software [12] with geometries first optimized by AM1 calculations [13] as starting structures.

Theoretical NMR chemical shifts were calculated by DFT at the B3LYP/6-311++G(2d,2p) level of theory using the GIAO method [14]. Geometry of the first excited state for compound (1) was calculated by means of CIS procedure (single excitation CI) [15]. The ZINDO method [16] was applied to interpret the UV–vis spectra of (1).

## 2.4. Synthesis of azomethines and ketimines (1)–(10)

9-Oxo-9,10-dihydroacridine-4-carboxylic acid hydrazide (0.39 mmol) was suspended in dry ethanol (10 mL) containing a few drops of concentrated HCl and to this was added the appropriate aldehyde or ketone (0.43 mmol). The reaction mixture was stirred at room temperature for 1 h (aldehydes) or 24 h (ketones) until a precipitant was evident that was then filtered off, washed with methanol, dried and then finally recrystallized from methanol. The experimental data for (1)–(10) are contained in Table 1 with the spectroscopic data presented in Tables 2–7.

Experimental and spectroscopic data are also reproduced in full in the Supplementary material.

## 3. Results and discussion

### 3.1. Synthesis

From 2,2'-iminodibenzoic acid, treatment with polyphosphoric acid yielded 9-oxo-9,10-dihydroacridine-4-carboxylic acid [7]. Subsequent esterification of this substrate with methyl iodide in DMF/NaH yielded the methyl ester, following which treatment with hydrazine monohydrate provided corresponding 9-oxo-9,10-dihydroacridine-4-carboxylic acid hydrazide [1]. The azomethines and ketimines (1)–(10) were then prepared generally in high yield by the condensation reaction of appropriate aldehydes and ketones accordingly with the prepared 9-oxo-9,10-dihydroacridine-4-carboxylic acid hydrazide with each product providing satisfactory elemental analysis. The azomethines (1)–(6) provided higher yields than the ketimines (9) and (10) which were significantly slower to react. For the *tert*-butyl azomethine (8) and, inexplicably, the methyl azomethine (7) lower, but still satisfactory, yields were obtained. The molecular structures of the synthesized compounds (1)–(10) were established and characterized spectroscopically by NMR ( $^1\text{H}$ ,  $^{13}\text{C}$ ,  $^{15}\text{N}$ , and 2D experiments), UV–vis, IR and fluorescence methods and by quantum chemical calculations using DFT at the B3LYP/6-311+G(d,p) level of theory and semiempirical ZINDO and AM1 methods.

### 3.2. Spectroscopic analysis

The analyses of the  $^1\text{H}$ ,  $^{13}\text{C}$  and  $^{15}\text{N}$  NMR, UV–vis, and FT-IR spectra for compounds (1)–(10) and the subsequent interpretations were compared with each other and then also with the conclusions drawn from quantum chemical calculations. For the assignment of the NMR signals, 1D and 2D NMR spectra were measured and

**Table 1**  
Experimental data for (1)–(10).

Cmpd	Yield, %	M.p., °C	Formula	Found C, H, N			Calcd C, H, N		
				C	H	N	C	H	N
(1)	85	301–302	C <sub>21</sub> H <sub>15</sub> N <sub>3</sub> O <sub>2</sub>	74.02	4.58	12.62	73.89	4.43	12.31
(2)	80	310–312	C <sub>21</sub> H <sub>14</sub> ClN <sub>3</sub> O <sub>2</sub>	67.69	3.96	11.43	67.12	3.75	11.18
(3)	90	>350	C <sub>22</sub> H <sub>17</sub> N <sub>3</sub> O <sub>3</sub>	71.23	4.75	11.43	71.15	4.61	11.31
(4)	90	326–328	C <sub>21</sub> H <sub>14</sub> BrN <sub>3</sub> O <sub>2</sub>	60.44	3.49	9.93	60.02	3.36	10.00
(5)	80	312–315	C <sub>21</sub> H <sub>13</sub> Cl <sub>2</sub> N <sub>3</sub> O <sub>2</sub>	61.35	3.28	9.91	61.48	3.19	10.24
(6)	80	309–312	C <sub>24</sub> H <sub>21</sub> N <sub>3</sub> O <sub>2</sub>	74.99	5.73	11.26	75.18	5.52	10.96
(7)	45	248–250	C <sub>16</sub> H <sub>13</sub> N <sub>3</sub> O <sub>2</sub>	68.48	4.42	15.21	68.81	4.69	15.04
(8)	48	271–273	C <sub>19</sub> H <sub>19</sub> N <sub>3</sub> O <sub>2</sub>	70.60	6.10	12.61	71.01	5.96	13.07
(9)	65	248–250	C <sub>22</sub> H <sub>17</sub> N <sub>3</sub> O <sub>2</sub>	74.87	4.63	11.58	74.35	4.82	11.82
(10)	65	247–250	C <sub>17</sub> H <sub>15</sub> N <sub>3</sub> O <sub>2</sub>	69.86	4.92	14.01	69.61	5.15	14.33

the ensuing assigned chemical shifts correlated with the corresponding values obtained using the GIAO model. UV–vis spectra of (1)–(10) were recorded in dimethyl acetamide (DMA) and *m*-cresol and then also additionally in methanol and dimethyl formamide (DMF) for compounds (1), (7), (9) and (10) to estimate the effect of solvent polarity and to evaluate protic vs. aprotic solvent effects. FT-IR spectra of the compounds (1)–(10) were acquired in KBr discs and, additionally for compounds (1) and (9), also in CS<sub>2</sub> solution for evaluation and consequent interpretation as well as to assess the state of hydrogen bonding in the molecules. The dependency on state was used to distinguish between intra- and intermolecular interactions, with conclusions also supported by vibrational analysis provided by molecular modeling.

### 3.2.1. NMR spectroscopy

The <sup>1</sup>H and <sup>13</sup>C NMR chemical shifts of the nuclei of the acridone skeleton were found to lie within the expected ranges in comparison to acridone [2,17–19], acridone derivatives [1] and also with acridine derivatives – except for the C-9 carbon – consisting of a dihydroacridine ring [20]. The results for compounds (1)–(10) are summarized in Table 2.

The chemical shifts of the ketonic carbons C-9 and the amino hydrogens H-10 of the acridone system were characteristically located in the regions 176.4–176.6 ppm and 11.66–11.99 ppm, respectively, and are in good agreement with the literature values for acridone (see footnote Table 2). The C-1' carbonyl carbons of the amide group in the side chain all resonated within the range 163.6–164.4 ppm whilst the amidic NH protons H-2' resonated in the 10.92–12.53 ppm range. The dominant state of tautomerism regarding the labile protons located at H-10 and H-2' was clear based on the one-bond correlations observed in <sup>1</sup>H–<sup>15</sup>N HSQC spectra for compounds (2), (4)–(6) and (10) but would have been evident in any case based on the observed chemical shifts for the acridone moiety [1,2,17–20]. The consistency of the diagnostic chemical shifts of the other compounds with those of (2), (4)–(6) and (10) confirms their identical tautomeric state. For example, in addition to the previously mentioned nuclei; C-4a and C-10a, 139–141 ppm; C-8a and C-9a, 118–122 ppm and, in particular [21,22], C-4 and C-5, 118–122 ppm for the acridone moiety and H-2', C-1' and C-4' for the side chain.

It was not possible to evaluate the predominance of the *E/Z* configurations relating to the imine N<sub>3</sub>=C<sub>4</sub>' double bond and also for the amide C<sub>1</sub>'–N<sub>2</sub>' bond based on the experimental NMR data alone. Clearly for both processes they were either very biased or consisted of rapidly interconverting equilibria. However, although not evident directly from the spectral data, indirect evidence for the predominant *E/Z* configurations, as well as for the gross structures and tautomeric states, was obtained from molecular modeling studies (*vide infra*). For the <sup>1</sup>H nuclei, calculation of the chemical shifts on optimized structures using the GIAO method at the B3LYP/6-311++G(2d,2p) level of theory yielded a

linear correlation when plotted against the experimental values:  $\delta_{\text{exp}} = 0.94 \times \delta_{\text{calc}} + 0.62$ , correlation coefficient  $r = 0.898$ . Better linear correlations are provided, though, if the non-labile and NH protons are treated separately due to the effect of the polar solvent [20,23,24]. For the <sup>13</sup>C nuclei, calculation of the chemical shifts also yielded a linear correlation when plotted against the experimental values:  $\delta_{\text{exp}} = 0.95 \times \delta_{\text{calc}} + 1.70$ , correlation coefficient  $r = 0.988$ . These results support the correctness of the assigned structures. Graphical representations of these results are presented in the Supplementary material.

Distinctions were apparent between the C-4' <sup>13</sup>C NMR chemical shifts for the azomethines (1)–(8) and ketimines (9) and (10) and they arise from the effects of the substituents on the imine C<sub>4</sub>'=N<sub>3</sub>' double bond. In general,  $\delta_{\text{C4'}}$  for azomethines (1)–(8) is shielded in comparison to ketimines (9) and (10). For example, 149.8 ppm is observed for  $\delta_{\text{C4'}}$  in the azomethine methyl derivative (7) whilst 161.6 ppm is instead obtained for the ketimine dimethyl derivative (10). An exception is the *tert*-butyl derivative (8) ( $\delta_{\text{C4'}} = 160.2$  ppm) for which C-4' is even more deshielded than in the ketimine phenyl methyl derivative (9) ( $\delta_{\text{C4'}} = 156.7$  ppm). However, these differences are not due to direct inductive effects by the substituents on the shielding of C-4', but rather by induced polarization changes to the imine C<sub>4</sub>'=N<sub>3</sub>' double bond [25]. This can be seen in Table 3 where there is a fair, though not perfectly sequenced, correlation between the atomic charges obtained from the DFT calculations for C-4' and the observed chemical shift. The same underlying cause is also responsible for the observed differences within the series (1)–(8).

In the <sup>15</sup>N NMR, the chemical shifts for the N-10 nitrogen of (2), (4)–(6) and (10) were all at ca. –268.6 ppm and are essentially unaffected by the side chain R and R' substituents (Table 4). The chemical shifts for the N-2' nitrogen range from –212.2 ppm for the ketimine derivative (10) to –202.5 ppm for azomethine (6), and for the N-3' nitrogen, from –73.9 ppm for ketimine (10) to –53.5 ppm for azomethine (6). The chemical shifts changes observed for the N-3' and N-2' nitrogens emphatically validate the assertion that polarizability changes to the imine C<sub>4</sub>'=N<sub>3</sub>' double bond are responsible for the chemical shift changes wrought on C-4'.

If inductive effects were solely responsible for the changes to C-4' then similar changes would be observed for both N-3' and N-2', but to lesser degrees. Of course N-3' should be subject to the same underlying cause as C-4' given that it is also obviously part of the imine C<sub>4</sub>'=N<sub>3</sub>' double bond. Implicitly, the changes observed on N-3' (Table 4) are comparable in range to C-4' (20.4 ppm vs. 17.0 ppm, respectively) but, incisively, they are in reverse order, as they should be if the imine C<sub>4</sub>'=N<sub>3</sub>' double bond is subjected to polarization changes. Thus, whilst C-4' in (10) is highly deshielded, this is contrasted by the relatively highly shielded position of its N-3' partner. N-2' will also be affected by the polarization of the imine C<sub>4</sub>'=N<sub>3</sub>' double bond since it is attached directly to N-3' and it should follow N-3' in terms of chemical shift changes as it too will

**Table 2**<sup>1</sup>H and <sup>13</sup>C NMR spectra of azomethines and ketimines (**1**)–(**10**).

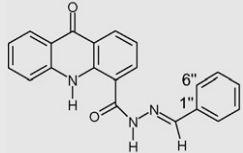
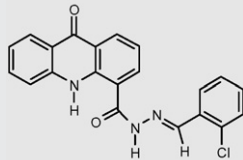
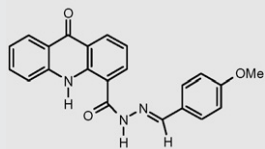
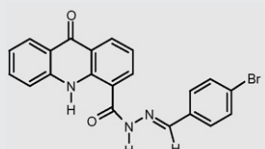
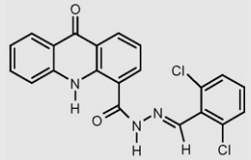
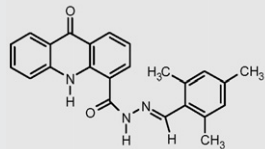
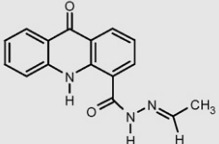
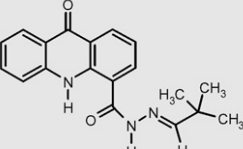
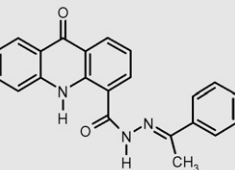
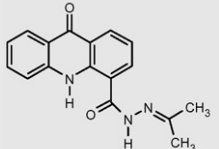
Structure	NMR, $\delta$ [ppm]
<p>(1)</p> 	<p><sup>1</sup>H NMR (DMSO-<i>d</i><sub>6</sub>, 400 MHz) <math>\delta</math> ppm: 12.26 (1H, s, H-2'), 11.81 (1H, s, H-10), 8.48 (1H, d, <i>J</i> = 7.2 Hz, H-1), 8.47 (1H, s, H-4'), 8.26 (1H, d, <i>J</i> = 7.2 Hz, H-3), 8.24 (1H, d, <i>J</i> = 7.6 Hz, H-8), 7.86 (1H, d, <i>J</i> = 8.4 Hz, H-5), 7.78 (3H, m, H-2'',6'',6), 7.49 (3H, m, H-3'',4'',5''), 7.40 (1H, t, <i>J</i> = 7.2 Hz, H-2), 7.32 (1H, m, H-7); <sup>13</sup>C NMR (DMSO-<i>d</i><sub>6</sub>, 100 MHz) <math>\delta</math> ppm: 176.4 (C-9), 163.8 (C-1'), 148.6 (C-4'), 140.2 (C-10a), 139.8 (C-4a), 134.0 (C-1''), 133.9 (C-6), 133.3 (C-3), 130.3 (C-4''), 130.2 (C-1), 128.9 (C-3'',5''), 127.1 (C-2'',6''), 125.7 (C-8), 121.9 (C-7), 121.4 and 118.9 (C-4, C-9a), 120.4 (C-8a), 119.9 (C-2), 118.5 (C-5)</p>
<p>(2)</p> 	<p><sup>1</sup>H NMR (DMSO-<i>d</i><sub>6</sub>, 400 MHz) <math>\delta</math> ppm: 12.46 (1H, s, H-2'), 11.85 (1H, s, H-10), 8.90 (1H, s, H-4'), 8.51 (1H, d, <i>J</i> = 8.0 Hz, H-1), 8.32 (1H, d, <i>J</i> = 7.2 Hz, H-3), 8.26 (1H, d, <i>J</i> = 8.0 Hz, H-8), 8.08 (1H, m, H-6'), 7.86 (1H, d, <i>J</i> = 8.4 Hz, H-5), 7.77 (1H, m, H-6), 7.56 (1H, m, H-3''), 7.51–7.45 (2H, m, H-4'',5''), 7.41 (1H, dd, <i>J</i> = 7.2, 8.0 Hz, H-2), 7.33 (1H, m, H-7); <sup>13</sup>C NMR (DMSO-<i>d</i><sub>6</sub>, 100 MHz) <math>\delta</math> ppm: 176.5 (C-9), 164.0 (C-1'), 144.6 (C-4'), 140.3 (C-10a), 140.0 (C-4a), 133.9 (C-6), 133.5 (C-3), 133.4 (C-1''), 131.7 (C-4''), 131.3 (C-2''), 130.5 (C-1), 130.0 (C-3''), 127.7 (C-5''), 126.8 (C-6''), 125.8 (C-8), 122.0 (C-7), 121.5 and 118.6 (C-4, C-9a), 120.5 (C-8a), 119.9 (C-2), 118.6 (C-5)</p>
<p>(3)</p> 	<p><sup>1</sup>H NMR (DMSO-<i>d</i><sub>6</sub>, 400 MHz) <math>\delta</math> ppm: 12.15 (1H, s, H-2'), 11.86 (1H, s, H-10), 8.48 (1H, d, <i>J</i> = 7.6 Hz, H-1), 8.42 (1H, s, H-4'), 8.26 (1H, m, H-3), 8.25 (1H, m, H-8), 7.86 (1H, d, <i>J</i> = 6.8 Hz, H-5), 7.78 (1H, m, H-6), 7.73 (2H, m, H-2'',6''), 7.40 (1H, dd, <i>J</i> = 7.6, 8.4 Hz, H-2), 7.33 (1H, m, H-7), 7.06 (2H, m, H-3'',5''), 3.82 (3H, s, OCH<sub>3</sub>); <sup>13</sup>C NMR (DMSO-<i>d</i><sub>6</sub>, 100 MHz) <math>\delta</math> ppm: 176.5 (C-9), 163.7 (C-1'), 161.0 (C-4''), 148.5 (C-4'), 140.2 (C-10a), 139.8 (C-4a), 133.9 (C-6), 133.2 (C-3), 130.1 (C-1), 128.8 (C-2'',6''), 126.6 (C-1''), 125.7 (C-8), 121.9 (C-7), 121.4 and 119.0 (C-4, C-9a), 120.4 (C-8a), 119.9 (C-2), 118.5 (C-5), 114.4 (C-3'',5''), 55.3 (OCH<sub>3</sub>)</p>
<p>(4)</p> 	<p><sup>1</sup>H NMR (DMSO-<i>d</i><sub>6</sub>, 400 MHz) <math>\delta</math> ppm: 12.35 (1H, s, H-2'), 11.82 (1H, s, H-10), 8.50 (1H, d, <i>J</i> = 8.4 Hz, H-1), 8.46 (1H, s, H-4'), 8.28–8.25 (2H, m, H-3,8), 7.86 (1H, m, H-5), 7.77 (1H, m, H-6), 7.73 (2H, m, H-2'',6''), 7.69 (2H, m, H-3'',5''), 7.40 (1H, dd, <i>J</i> = 7.2, 8.4 Hz, H-2), 7.33 (1H, m, H-7); <sup>13</sup>C NMR (DMSO-<i>d</i><sub>6</sub>, 100 MHz) <math>\delta</math> ppm: 176.4 (C-9), 163.9 (C-1'), 147.3 (C-4'), 140.2 (C-10a), 139.8 (C-4a), 133.9 (C-6), 133.3 (C-3), 131.9 (C-3'',5''), 131.1 (C-1''), 130.3 (C-1), 129.0 (C-2'',6''), 125.7 (C-8), 123.5 (C-4''), 121.9 (C-7), 121.4 and 118.9 (C-4, C-9a), 120.4 (C-8a), 119.9 (C-2), 118.4 (C-5)</p>
<p>(5)</p> 	<p><sup>1</sup>H NMR (DMSO-<i>d</i><sub>6</sub>, 400 MHz) <math>\delta</math> ppm: 12.53 (1H, s, H-2'), 11.89 (1H, s, H-10), 8.74 (1H, s, H-4'), 8.52 (1H, d, <i>J</i> = 7.2 Hz, H-1), 8.36 (1H, d, <i>J</i> = 6.8 Hz, H-3), 8.25 (1H, d, <i>J</i> = 7.6 Hz, H-8), 7.86 (1H, d, <i>J</i> = 8.0 Hz, H-5), 7.77 (1H, m, H-6), 7.60 (2H, d, <i>J</i> = 6.8 Hz, H-3'',5''), 7.48 (1H, t, <i>J</i> = 6.8 Hz, H-4''), 7.42 (1H, dd, <i>J</i> = 6.8, 7.2 Hz, H-2), 7.33 (1H, m, H-7); <sup>13</sup>C NMR (DMSO-<i>d</i><sub>6</sub>, 100 MHz) <math>\delta</math> ppm: 176.5 (C-9), 164.1 (C-1'), 144.3 (C-4'), 140.2 (C-4a), 140.2 (C-10a), 134.0 (C-3), 134.0 (C-6), 133.7 (C-2'',6''), 131.4 (C-4''), 130.8 (C-1), 130.2 (C-1''), 129.2 (C-3'',5''), 125.8 (C-8), 122.1 (C-7), 121.6 and 118.1 (C-4, C-9a), 120.5 (C-8a), 119.9 (C-2), 118.6 (C-5)</p>
<p>(6)</p> 	<p><sup>1</sup>H NMR (DMSO-<i>d</i><sub>6</sub>, 400 MHz) <math>\delta</math> ppm: 12.09 (1H, s, H-2'), 11.99 (1H, s, H-10), 8.84 (1H, s, H-4'), 8.51 (1H, d, <i>J</i> = 8.0 Hz, H-1), 8.34 (1H, d, <i>J</i> = 7.2 Hz, H-3), 8.25 (1H, d, <i>J</i> = 7.6 Hz, H-8), 7.88 (1H, d, <i>J</i> = 8.8 Hz, H-5), 7.76 (1H, m, H-6), 7.42 (1H, dd, <i>J</i> = 7.2, 8.0 Hz, H-2), 7.33 (1H, m, H-7), 6.96 (2H, s, H-3'',5''), 2.51 (6H, s, CH<sub>3</sub>-2'',6''), 2.27 (3H, s, CH<sub>3</sub>-4''); <sup>13</sup>C NMR (DMSO-<i>d</i><sub>6</sub>, 100 MHz) <math>\delta</math> ppm: 176.4 (C-9), 163.6 (C-1'), 149.1 (C-4'), 140.1 (C-10a), 138.6 (C-4a), 137.6 (C-2'',6''), 133.9 (C-6), 133.3 (C-3), 130.3 (C-1), 129.5 (C-3'',5''), 127.7 (C-1''), 125.7 (C-8), 122.0 (C-7), 121.5 and 118.3 (C-4, C-9a), 120.4 (C-8a), 119.9 (C-2), 118.6 (C-5), 21.1 (CH<sub>3</sub>-2'',6''), 20.6 (CH<sub>3</sub>-4'')</p>



Table 2 (Continued)

Structure	NMR, $\delta$ [ppm]
 <p>(7)</p>	<sup>1</sup> H NMR (DMSO- <i>d</i> <sub>6</sub> , 400 MHz) $\delta$ ppm: 11.86 (1H, s, H-2'), 11.81 (1H, s, H-10), 8.46 (1H, d, <i>J</i> = 8.0 Hz, H-1), 8.24 (1H, d, <i>J</i> = 8.4 Hz, H-8), 8.18 (1H, d, <i>J</i> = 7.2 Hz, H-3), 7.83–7.72 (2H, m, H-5,6), 7.80 (1H, m, H-4'), 7.37 (1H, dd, <i>J</i> = 7.2, 8.0 Hz, H-2), 7.32 (1H, m, H-7), 1.99 (3H, d, <i>J</i> = 5.6 Hz, CH <sub>3</sub> ); <sup>13</sup> C NMR (DMSO- <i>d</i> <sub>6</sub> , 100 MHz) $\delta$ ppm: 176.5 (C-9), 163.6 (C-1'), 149.8 (C-4'), 140.2 (C-10a), 139.9 (C-4a), 133.9 (C-6), 133.2 (C-3), 130.0 (C-1), 125.8 (C-8), 121.9 (C-7), 121.4 and 119.0 (C-4, C-9a), 120.4 (C-8a), 119.9 (C-2), 118.5 (C-5), 18.5 (CH <sub>3</sub> )
 <p>(8)</p>	<sup>1</sup> H NMR (DMSO- <i>d</i> <sub>6</sub> , 400 MHz) $\delta$ ppm: 11.82 (1H, s, H-10), 11.78 (1H, s, H-2'), 8.46 (1H, d, <i>J</i> = 7.2 Hz, H-1), 8.24 (1H, d, <i>J</i> = 8.0 Hz, H-3), 8.20 (1H, d, <i>J</i> = 7.6 Hz, H-8), 7.86 (1H, d, <i>J</i> = 8.0 Hz, H-5), 7.76 (1H, m, H-6), 7.74 (1H, s, H-4'), 7.36 (1H, dd, <i>J</i> = 7.2, 8.0 Hz, H-2), 7.32 (1H, m, H-7), 1.14 (9H, s, CH <sub>3</sub> ); <sup>13</sup> C NMR (DMSO- <i>d</i> <sub>6</sub> , 100 MHz) $\delta$ ppm: 176.5 (C-9), 163.7 (C-1'), 160.2 (C-4'), 140.3 (C-10a), 139.9 (C-4a), 133.9 (C-6), 133.2 (C-3), 130.0 (C-1), 125.7 (C-8), 121.9 (C-7), 121.4 and 119.0 (C-4, C-9a), 120.4 (C-8a), 119.9 (C-2), 118.5 (C-5), 34.8 (C <sub>q</sub> - <i>t</i> -Bu), 27.1 (CH <sub>3</sub> )
 <p>(9)</p>	<sup>1</sup> H NMR (DMSO- <i>d</i> <sub>6</sub> , 400 MHz) $\delta$ ppm: 11.66 (1H, s, H-10), 11.21 (1H, s, H-2'), 8.48 (1H, d, <i>J</i> = 7.6 Hz, H-1), 8.25 (2H, m, H-3,8), 7.92 (2H, m, H-2'',6''), 7.87 (1H, m, H-5), 7.75 (1H, m, H-6), 7.47 (3H, m, H-3'',4'',5''), 7.39 (1H, m, H-2), 7.32 (1H, m, H-7), 2.43 (3H, s, CH <sub>3</sub> ); <sup>13</sup> C NMR (DMSO- <i>d</i> <sub>6</sub> , 100 MHz) $\delta$ ppm: 176.6 (C-9), 164.4 (C-1'), 156.7 (C-4'), 140.4 (C-10a), 139.8 (C-4a), 137.9 (C-1''), 134.1 (C-3), 133.9 (C-6), 130.0 (C-1), 129.6 (C-4''), 128.4 (C-3'',5''), 126.5 (C-2'',6''), 125.8 (C-8), 121.9 (C-7), 121.4 and 119.9 (C-4, C-9a), 120.4 (C-8a), 120.0 (C-2), 118.6 (C-5), 14.8 (CH <sub>3</sub> )
 <p>(10)</p>	<sup>1</sup> H NMR (DMSO- <i>d</i> <sub>6</sub> , 400 MHz) $\delta$ ppm: 11.71 (1H, s, H-10), 10.92 (1H, s, H-2'), 8.43 (1H, d, <i>J</i> = 7.6 Hz, H-1), 8.23 (1H, d, <i>J</i> = 8.0 Hz, H-8), 8.17 (1H, m, H-3), 7.81 (1H, d, <i>J</i> = 8.0 Hz, H-5), 7.38 (1H, m, H-6), 7.34 (1H, m, H-2), 7.30 (1H, m, H-7), 2.05 (3H, s, CH <sub>3</sub> ), 1.99 (3H, s, CH <sub>3</sub> ); <sup>13</sup> C NMR (DMSO- <i>d</i> <sub>6</sub> , 100 MHz) $\delta$ ppm: 176.6 (C-9), 163.9 (C-1'), 161.6 (C-4'), 140.3 (C-10a), 139.7 (C-4a), 133.9 (C-6), 133.6 (C-3), 129.7 (C-1), 125.8 (C-8), 121.9 (C-7), 121.4 and 119.7 (C-4, C-9a), 120.4 (C-8a), 120.0 (C-2), 118.5 (C-5), 25.2 (CH <sub>3</sub> ), 18.3 (CH <sub>3</sub> )

Additional compounds for reference purposes were also examined: acridone: C-9, 176.8 ppm (lit. 176.4 [2] and 176.7 ppm [19]); H-10, 11.81 ppm (lit. 11.70 [2] and 11.72 ppm [17]); an anomalous chemical shift value 9.61 ppm has also been reported [18]); 4-methyl acridone: C-9, 177.0 ppm; H-10, 10.62 ppm; acridone-4-carboxylic acid: C-9, 176.5 ppm; H-10, 13.15 ppm; C-1', 169.2 ppm; benzoic acid (1-phenyl-methylidene) hydrazide: C(=O), 163.6 ppm; C(=N), 148.3 ppm; H(N), 11.86 ppm; (=CPh)H, 8.50 ppm; benzoic acid (1-phenyl-ethylidene) hydrazide: C(=O), 163.9 ppm; C(=N), 155.5 ppm; H(N), 10.76 ppm.

be subject to similar electron density changes but obviously the size of its changes should be muted, as they indeed are. Only derivative (6) deviates significantly from the otherwise clear correlation and association and this is evident for both N-3' and N-2' nitrogens as a pair with respect to the C-4' carbon in this compound. With respect to the calculated atomic charges on the nitrogens (Table 4), the correlation is also again only fair for the N-3' nitrogen, though

notably the strong effect observed on N-3' in (10) is replicated by the calculations relative to the other available shifts. For this same set of compounds, (2), (4)–(6) and (10), the correlation of  $\delta_{C4'}$  and  $Q_{C4'}$  is fair with only derivatives (2) and (5) out of sequence and (4) and (6) out of sequence. The sequence order for N-2' is perfect, and also with a large differential to derivative (10) relative to the other compounds.

**Table 3**  
C-4' <sup>13</sup>C NMR chemical shifts and DFT-calculated atomic charges for (1)–(10).

Cmpd	(1)	(2)	(3)	(4)	(5)	(6)	(7)	(8)	(9)	(10)
$\delta_{C4'}$	148.6	144.6	148.5	147.3	144.3	149.1	149.8	160.2	156.7	161.6
$Q_{C4'}$	−0.83	−1.11	−0.37	−0.67	−1.56	−1.07	−0.07	−0.35	−0.40	+0.04

**Table 4**  
<sup>15</sup>N and C-4' <sup>13</sup>C NMR chemical shifts and atomic charges for (2), (4)–(6) and (10).

Cmpd	$\delta_{N10}$	$\delta_{N2'}$	$\delta_{N3'}$	$\delta_{C4'}$	$Q_{N2'}$	$Q_{N3'}$
(2)	−268.5	−203.3	−55.1	144.6	−0.113	+0.110
(4)	−268.5	−204.4	−58.7	147.3	−0.150	+0.114
(5)	−268.5	−202.8	− <sup>a</sup>	144.8	−0.103	+0.184
(6)	−268.5	−202.5	−53.5	149.1	−0.089	+0.084
(10)	−268.7	−212.2	−73.9	161.6	−0.238	+0.026

<sup>a</sup> Correlations were not observed even for assorted parameters.

**Table 5**Infrared spectral data<sup>a</sup> (KBr discs) for (1)–(10).

Cmpd	$\nu(\text{N}_{10}-\text{H})$ , acridone	$\nu(\text{N}_{2'}-\text{H})$ , amide	$\nu(\text{C}-\text{H})$ , aromatic	$\nu(\text{C}_9=\text{O})$ , acridone	$\nu(\text{C}_{1'}=\text{O})$ , amide	$\nu(\text{C}_4=\text{N})$	$\delta(\text{N}-\text{H})$
(1)	3260	3155	3063	1661	1617	1596	1573
(2)	3351	3212	3053	1647	1616	1594	1572
(3)	3265 <sup>b</sup>	— <sup>c</sup>	3060	1670	1619	1600	1575
(4)	3262 <sup>b</sup>	— <sup>c</sup>	3060	1670	1622	1594	1570
(5)	3313	3205	3044	1654	1613	1591	1578
(6)	3279	3232	3064	1647	1616	1592	1573
(7)	3286	3194	3026	1645	1620	1601	1572
(8)	3265	3170	3006	1663	1628	1594	1570
(9)	3286	3172	3061	1663	1618	1592	1578
(10)	3288	3196	3025	1641	1619	1597	1565

<sup>a</sup> Frequencies in  $\text{cm}^{-1}$ .<sup>b</sup> Broad.<sup>c</sup> Overlapped.

### 3.2.2. Infrared spectroscopy

Selected IR bands (KBr discs) and assignments for (1)–(10) are presented in Table 5 with full documentation of the IR data presented in the Supplementary material. Bands assigned to the amidic group  $\nu(\text{N}_{2'}-\text{H})$  stretch were observed in the region 3232–3155  $\text{cm}^{-1}$  analogously to model benzaldehyde benzoylhydrazone (3199–3153  $\text{cm}^{-1}$ , KBr disc) whilst bands in the 3351–3260  $\text{cm}^{-1}$  region were attributed to the  $\nu(\text{N}_{10}-\text{H})$  stretch where H-10 of the acridone skeleton is intramolecularly hydrogen bonded to the O-1' oxygen of the amide carbonyl group in accordance with our previous study [26]. This assignment is consistent with  $\nu(\text{N}_{10}-\text{H})$  stretch in model methyl 9-oxo-9,10-dihydroacridine-4-carboxylate at 3269  $\text{cm}^{-1}$  (KBr disc). Stretching vibrations,  $\nu(\text{C}-\text{H})$ , of the aromatic C–H bonds were present in the region 3064–3006  $\text{cm}^{-1}$  whilst bands in the region 1601–1591  $\text{cm}^{-1}$  were assigned to the stretching vibrations,  $\nu(\text{C}_4=\text{N})$ , of the imine  $\text{C}_4=\text{N}$  double bond. Bending vibrations for the N–H bonds,  $\delta(\text{N}-\text{H})$ , were present within the range 1578–1565  $\text{cm}^{-1}$ .

Each of the compounds (1)–(10) also possesses two characteristic vibrational frequencies for the acridone and amide carbonyl groups in the 1670–1641  $\text{cm}^{-1}$  and 1628–1613  $\text{cm}^{-1}$  regions, respectively. The lower than usual values for the acridone  $\nu(\text{C}_9=\text{O})$

stretching frequency compared to the typical values for ketones (ca. 1700  $\text{cm}^{-1}$ ) are nevertheless in accordance with our calculations (Table 1, Supplementary material) and calculations [27] for model compounds acridone {calculated for the free molecule, 1659  $\text{cm}^{-1}$ ; calculated for hydrogen-bonded dimer, 1629  $\text{cm}^{-1}$ ; observed, 1635  $\text{cm}^{-1}$  (in KBr)} and 9,10-anthraquinone (calculated, 1672  $\text{cm}^{-1}$ ).

In order to confirm the presence and assignments of both intra- and intermolecular hydrogen bonding, compounds (1) and (9) were also examined in  $\text{CS}_2$ .

For compound (1) in  $\text{CS}_2$ , the broad band at 3441  $\text{cm}^{-1}$ , whose intensity decreased upon dilution, was assigned to the acridone  $\nu(\text{N}_{10}-\text{H})$  bond intermolecularly H-bonded to 2'-carbonyl of other molecule (see Section 3.3.3). Amidic  $\nu(\text{N}_{2'}-\text{H})$  bands corresponding to four possible conformers (amide *s-cis/s-trans* and imino *syn/anti* [28]) were observed at lower wavenumbers, including the sharp band at 3261  $\text{cm}^{-1}$  and anomalously split  $\nu(\text{N}_{2'}-\text{H})$  bands at 3191, 3153, and 3138  $\text{cm}^{-1}$  due to Fermi resonance. It is assumed that as a consequence of the hydrogen bonding present in this compound, amidic  $\nu(\text{N}_{2'}-\text{H})$  stretch is diminished sufficiently in wavenumber to approach the two combination bands at 3191 [ $\nu(\text{C}_{1'}=\text{O}) + \delta(\text{N}-\text{H})$ ] and 3153  $\text{cm}^{-1}$  [ $\nu(\text{C}_4=\text{N}) + \delta(\text{N}-\text{H})$ ], thereby leading to the occurrence of Fermi resonance [29–31]. The  $\nu(\text{N}_{2'}-\text{H})$

**Table 6**

UV–vis absorption maxima for (1)–(10).

Cmpd <sup>a</sup>	<i>m</i> -Cresol				DMA							
	$\lambda_{\text{max}1}$ (nm)	$\log \varepsilon_1$	$\lambda_{\text{max}2}$ (nm)	$\log \varepsilon_2$	$\lambda_{\text{max}1}$ (nm)	$\log \varepsilon_1$	$\lambda_{\text{max}2}$ (nm)	$\log \varepsilon_2$	$\lambda_{\text{max}3}$ (nm)	$\log \varepsilon_3$	$\lambda_{\text{max}4}$ (nm)	$\log \varepsilon_4$
(1)	310	4.49	422	4.35	307	4.84	402	4.57	456	3.72	484	3.75
(2) <sup>b</sup>	321	4.49	425	4.32	308	4.98	402	4.71	458	3.99	487	4.02
(3)	318	4.52	424	4.38	314	4.82	402	4.54	454	3.72	481	3.75
(4) <sup>b</sup>	320	4.32	425	4.16	309	5.06	402	4.75	458	3.95	486	3.98
(5)	308	4.65	424	4.48	302	4.57	406	4.41	457	3.55	485	3.56
(6)	315	4.38	421	4.33	307	4.59	402	4.25	453	3.61	481	3.64
(7)	301	4.19	420	4.18	294	4.77	401	4.70	446	3.27	475	3.20
(8)	305	4.64	419	4.69	291	4.68	405	4.59	454	3.93	481	3.98
(9)	310	4.62	421	4.53	298	4.79	403	4.61	448	3.69	475	3.71
(10)	303	4.58	420	4.61	300	4.78	401	4.30	450	3.69	477	3.71

Acridone in methanol:  $\lambda_{\text{max}}$ : 251, 295, 379, 397;  $\lambda_{\text{max}}$ : 251, 295, 381, 400 [41].<sup>a</sup> Concentration,  $1.25 \times 10^{-5}$  M.<sup>b</sup> Concentration for the DMA measurements,  $6.25 \times 10^{-6}$  M.**Table 7**Fluorescence spectral data<sup>a</sup> for (1)–(10).

Cmpd	(1)	(2)	(3)	(4)	(5)	(6)	(7)	(8)	(9)	(10)
$\lambda_{\text{em}}$ (nm)	446	455	448	453	440	445	443	448	455	443
$F$ (a.u.)	170	61	125	102	292	132	125	124	74	105
$F/F_0$ <sup>b</sup>	0.50	0.18	0.37	0.30	0.86	0.39	0.37	0.36	0.22	0.31

<sup>a</sup> Spectral width, 420–550 nm;  $\lambda_{\text{em}}$ , 410 nm.<sup>b</sup> Relative fluorescence, where  $F_0$  = fluorescence of 9-isothiocyanatoacridine in methanol ( $\lambda_{\text{em}}$ , 455 nm; concentration,  $2.75 \times 10^{-5}$  M) [1].

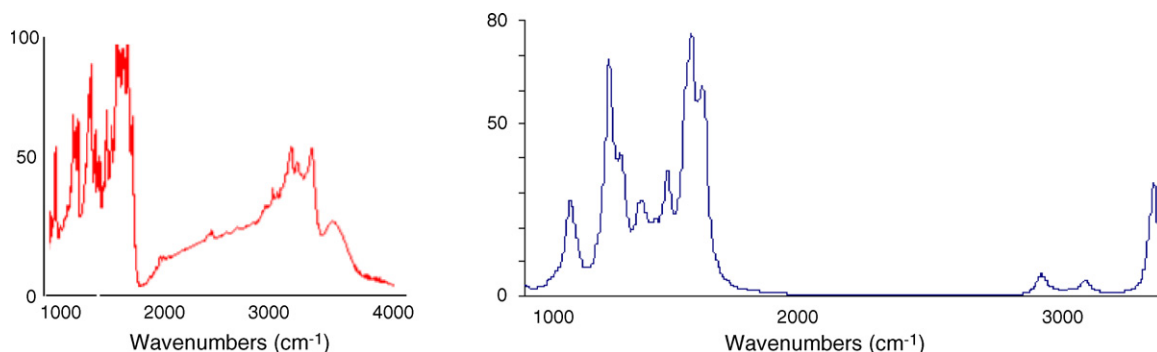


Fig. 2. Experimental (left) and DFT-calculated (right) IR spectra of methyl azomethine (7).

stretching band is also affected by the second harmonic vibration of  $\delta(\text{N-H})$  at  $3138\text{ cm}^{-1}$ , resulting in an interaction involving the combination of four vibrational energy levels. Fermi resonance is known to play an important role not only in the behavior of strong, but also of weak hydrogen bonds [32,33]. However, to estimate the strength of the hydrogen bonds it is necessary to obtain the frequencies of the bands unperturbed by Fermi resonance because only these are wholly dependent on force constants [34]. Unfortunately, relationships pertaining to four-level interactions have not so far been described in the literature for the calculation of Fermi resonance-corrected frequencies [35].

For compound (9) in  $\text{CS}_2$ , similarly as per (1), the broad band at  $3454\text{ cm}^{-1}$  decreasing upon dilution was assigned to the acridone  $\nu(\text{N}_{10}\text{-H})$  stretch whilst the split one at  $3286$  and  $3269\text{ cm}^{-1}$  and the bands at  $3200$ ,  $3168$ , and  $3141\text{ cm}^{-1}$  interacting by Fermi resonance to the amidic  $\nu(\text{N}_2\text{-H})$  stretch. Splitting of  $\nu(\text{N}_2\text{-H})$  bands was assigned to an intramolecular hydrogen bonding between the H-2' of the amide and the phenyl ring, which can be formed due to conformational freedom in the side chain. The band at  $3200\text{ cm}^{-1}$  was assigned to the combination band  $\nu(\text{C}_1=\text{O}) + \delta(\text{N-H})$ ; the band lying at  $3168\text{ cm}^{-1}$  belongs to the combination band  $\nu(\text{C}_4=\text{N}) + \delta(\text{N-H})$ ; whilst the band at  $3141\text{ cm}^{-1}$  is the overtone of the  $\delta(\text{N-H})$  vibration. Thus, similarly to (1) and for the same reasons, the band frequencies unperturbed by Fermi resonance were not able to be extracted to enable an estimation of the strength of the intramolecular hydrogen bond. The overtone of the  $\nu(\text{C}_1=\text{O})$  stretch of the hydrogen bonded amide carbonyl was also observed at  $3233\text{ cm}^{-1}$ .

The IR spectra of compounds (1)–(10) were simulated using DFT at the B3LYP/6-311+G(d,p) level of theory with the results for compound (7) presented in Fig. 2 and the results for all compounds tabulated in Supplementary material. The experimental frequencies were found to be reproduced well by the DFT calculations.

### 3.2.3. UV–vis spectroscopy

Two strong absorption bands within the ranges  $301\text{--}321\text{ nm}$  ( $\lambda_{\text{max}1}$ ,  $\log \varepsilon_1 > 4$ ) and  $419\text{--}425\text{ nm}$  ( $\lambda_{\text{max}2}$ ,  $\log \varepsilon_2 > 4$ ) were observed in the UV–vis spectra of azomethines and ketimines (1)–(10) in the non-polar, protic solvent *m*-cresol (dielectric constant,  $\varepsilon = 11.8$ ) (see Fig. 3 and Table 6). These bands are typical for acridone derivatives but whilst  $\lambda_{\text{max}1}$  is hypsochromically shifted in comparison to the spectrum of acridone itself,  $\lambda_{\text{max}2}$  is bathochromically shifted. In the polar, aprotic solvent DMA ( $\varepsilon = 37.8$ ), the first absorption band lies in the range  $291\text{--}314\text{ nm}$  ( $\log \varepsilon_1 > 4$ ) whilst the second absorption band is located in a narrow spectral range  $401\text{--}406\text{ nm}$  ( $\log \varepsilon_2 > 4$ ) (see Fig. 3 and Table 6). Thus, both bands are slightly hypsochromically shifted in comparison to *m*-cresol and furthermore, both bands exhibit a sizeable increase in the value of  $\log \varepsilon$ . In addition, weaker bands at longer wavelengths ( $\log \varepsilon_3$ ,  $\log \varepsilon_4 < 4$ ) were evident in DMA that were not present in *m*-cresol. To confirm these findings, UV–vis data for compounds (1), (7), (9) and (10) were also collected in the protic solvent methanol ( $\varepsilon = 32.6$ ) and the aprotic DMF ( $\varepsilon = 38.3$ ) and these results are tabulated in the Supplementary material together with graphical representations. From these results it was concluded that protic solvents suppress bands 3 and 4. The hypsochromic shifts for bands 1 and 2 concomitant with an increase in the value of  $\log \varepsilon$  observed upon changing from *m*-cresol to DMA, DMF or methanol could arise from solvent polarity and/or solvent aromaticity differences (*vide infra*). Significant differences between the polar solvents for bands 1 and 2 were not evident, and also of note, the absorption bands are only minimally affected by the substituents R and R'.

To gain greater insight into these observations, DFT and semiempirical ZINDO and AMI calculations were applied to phenyl derivative (1) as a representative example. For the ZINDO calculations, the theoretical data ( $\lambda_{\text{max}}$  and oscillator strength,  $f$ ) were found to be in good qualitative agreement with the experimental values after applying a scaling factor of 1.37. The calculations

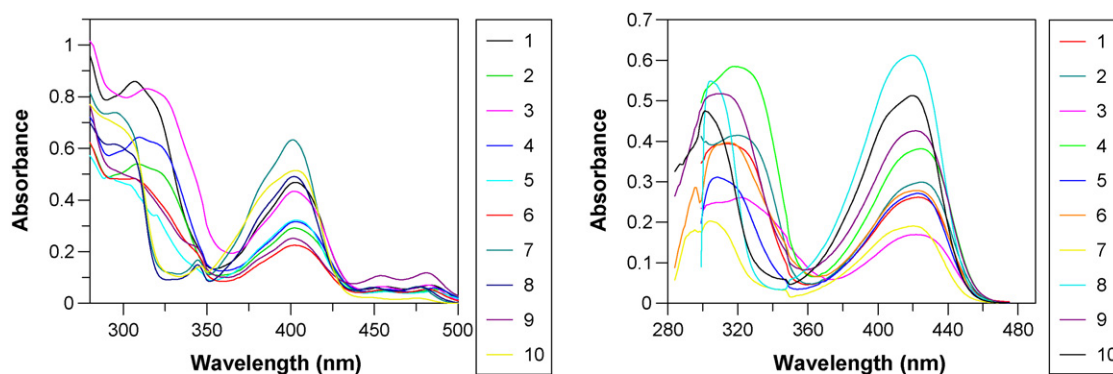


Fig. 3. UV–vis spectra of compounds (1)–(10) measured in DMA (left) and *m*-cresol (right).



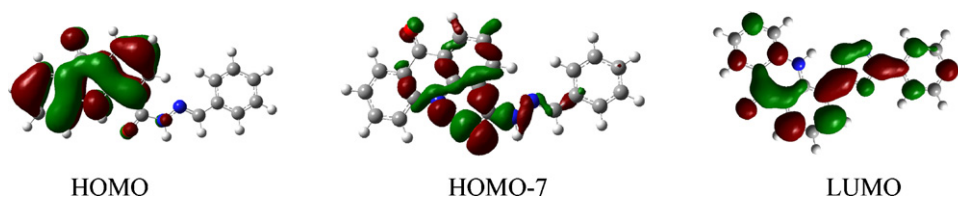


Fig. 4. Molecular orbitals calculated by the ZINDO method.

revealed that the  $\pi$ -system for HOMO, HOMO-1 and HOMO-2 is spread over the acridone skeleton, only to a minor extent over the side chain and not at all over the phenyl substituent. However, for LUMO, LUMO-1 and LUMO-2, the  $\pi$ -system is complex and spreads over the entire molecular framework. The strong bands predicted to occur at 334 ( $f=0.68$ ), 345 ( $f=0.77$ ) and 400 nm ( $f=0.55$ ) can be ascribed to the  $\pi \rightarrow \pi^*$  transitions from HOMO, HOMO-1 and HOMO-2 to LUMO, LUMO-1 and LUMO-2. The less intense, but nevertheless, significant complex band at 477 nm ( $f=0.023$ ) corresponds mainly to transitions from HOMO-7 to LUMO, LUMO-1, LUMO-2 and other higher orbitals.

HOMO-7 is formed mainly by lone electron pairs from the heteroatoms in the side chain, but also partially by acridone atomic orbitals (Fig. 4). The excitation arises mainly from these lone pairs to the LUMO and higher orbitals. The disappearance of longer wavelength bands in the protic solvents methanol and *m*-cresol (e.g. bands for (1) appear at 483 and 484 nm in DMF and DMA, respectively) is consistent with this interpretation as their extinction results from the interaction of the lone electron pairs of the side chain heteroatoms in both the ground and excited states with the solvent molecules.

Though generally upon moving to polar solvents,  $\pi \rightarrow \pi^*$  transitions are usually bathochromically shifted whilst the  $n \rightarrow \pi^*$  and  $n \rightarrow \sigma^*$  transitions are usually hypsochromically shifted [36], the experimentally observed hypsochromic shift in the polar solvents nevertheless indicates either destabilization by the solvent molecules of the excited state or stabilization of the ground state. DFT calculations revealed the excited state of (1) to be slightly less polar in comparison to the ground state of (1) (dipole moments were 6.5 and 6.3 D for the ground and the first excited states, respectively; for charges and geometry calculated using B3LYP/6-311+G(d,p), see Supplementary material). The influence of the solvent is to cause structural (geometrical and electronic) changes to the molecule to accommodate the environment and for more polar solvents, the new environment is favored by an increase in the solute's dipole moment. For a structure with a lower starting value for its dipole moment, resultant larger changes will occur (i.e. the excited state should be relatively destabilized by a polar solvent) leading to a larger increase in the energy level. A greater increase in the energy level in the excited state will thereby lead to an overall hypsochromic shift, as was observed upon a change of solvent from non-polar (*m*-cresol) to polar (DMA, DMF or methanol). An alternative or additional explanation for the observed result may be due to stacking-type interactions between the acridinone moiety of the compounds and the solvent *m*-cresol due to the aromatic nature of both entities, in essence similar to the ASIS effect that is observed in NMR. That is, the changes can be viewed in terms of aromatic vs. aliphatic solvents rather than in terms of solvent polarity. Evidently then, the excited state could be relatively stabilized by *m*-cresol thereby giving rise to the observed bathochromic shifts (with respect to the aliphatic solvents).

### 3.2.4. Fluorescence properties

The fluorescence of compounds (1)–(10) were measured in methanol and compared to the standard reference compound 9-isothiocyanatoacridine as per our previous works [37–39]. Table 7

contains the spectral data whilst the results are also portrayed graphically in Fig. 5. Of note, the spectra are all uniform and each only displays a single emission maximum. Unfortunately, an identifiable trend could not be discerned for the compounds with respect to the electron withdrawing/donating capabilities of the substituents and their ring positions in the case of aromatic-containing compounds as had been anticipated based on previous experience [1] and given the access between the substituents and the acridone system provided by conjugation within the side chain. Although this presumption of facile conjugation is challenged by the results of the molecular modeling study (*vide infra*). It is assumed therefore that combinations of polar and steric effects in addition to inductive effects are responsible for the observed differences [37]. Nevertheless, characteristic and comparable, especially for (5), fluorescence was obtained for the compounds with respect to 9-isothiocyanatoacridine thereby underlying their potential utility as biomarkers.

### 3.3. Molecular modeling

The imine  $N_3=C_4$  double bond, the amide group and the single bonds present in the side chains of (1)–(10) enable the existence of various *E/Z* isomers, tautomers and a wealth of conformational diversity in addition to the structural permutations available from the various moieties present in the compounds. The first goal of the modeling was to search the optimal geometries and find the most stable structures. The second goal was to examine the potential tautomerism in these compounds whilst the final aim was to evaluate the state of hydrogen bonding between the carbonyl oxygen and the NH protons, both intra- and intermolecularly.

#### 3.3.1. Optimized molecular structures

The molecular structures of (1)–(10) were first optimized by semiempirical AM1 calculations after which the obtained geometries were treated further using DFT at the B3LYP/6-311+G(d,p) level of theory. The calculations revealed that for an isolated

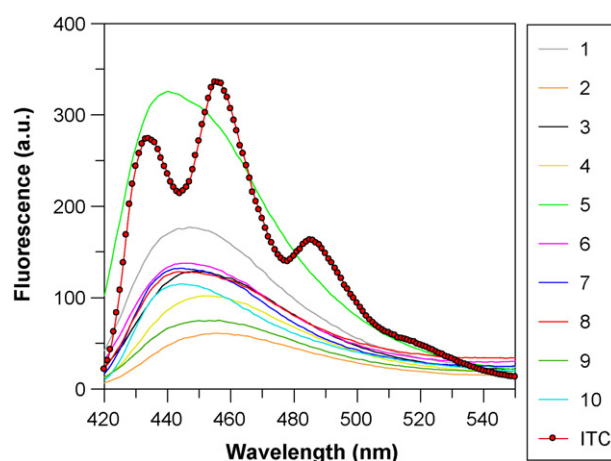


Fig. 5. The fluorescence spectra of (1)–(10) and the reference 9-isothiocyanatoacridine.

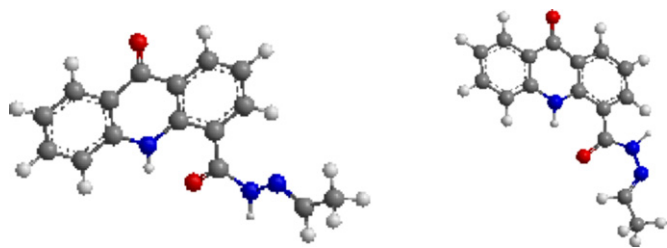


Fig. 6. The *EE* (left) and *EZ* (right) structures of (7).

molecule in the gas phase, for both azomethines and ketimines, the most stable structure in each case, the global minimum, has an *E* configuration for the imine  $N_3=C_4$  double bond and also an *E* configuration for the amide  $C_1'-N_2'$  bond. The structure, termed *EE*, is illustrated in Fig. 6 for the methyl derivative (7). Also portrayed in Fig. 6 is another low-energy structure, termed *EZ*, which is essentially almost equal in energy to *EE*,  $\Delta E$  between them being only 0.08 kcal/mol. In relation to the two structures, rotation is evident about the  $N_2'-N_3$  bond and also about the amide  $C_1'-N_2'$  bond, hence the configuration with respect to the amide linkage changes from *E* to *Z* in going from structure *EE* to structure *EZ*. Of note, for a simple configurational change along the amide bond, i.e. rotation about the  $C_1'-N_2'$  bond, energy barriers  $\Delta E$ s of 9.86–10.90 kcal/mol were obtained by AM1 calculations. It is also worth noting that the elongated side chain is slightly out of the plane of the acridone plane and the dihedral angles  $C_3-C_4-C_1'-N_2'$  are about 21 and 24° for the *EE* and *EZ* structures, respectively, thus in part explaining the lack of a correlation in the fluorescence spectra with respect to the substituents due to diminished conjugation. To put the small energy difference between *EE* and *EZ* into perspective, even the rotational states of the methyl group (based on the DFT calculations) were found to have an impact.

For the various local minima structures of (7) that were considered, the DFT-calculated  $\Delta E$ s span the range 0.08–8.71 kcal/mol above that of the global minimum. The single bonds  $C_4-C_1'$  and  $N_2'-N_3$  in particular in (1)–(10) enable the occurrence of a number of low-energy rotamers {see [Supplementary material](#) for rotational energy barriers calculated by AM1 for compounds (1)–(10)}. For example, for rotation angles of 42–50° about the  $C_4-C_1'$  bond, rotational energy barriers of only 2.69–2.97 kcal/mol were obtained. For rotation angles of 107–115° about the  $N_2'-N_3$  bond, larger rotational energy barriers of 7.49–8.32 kcal/mol, though, were obtained. It is interesting that one rotation about one bond such as the  $C_4-C_1'$  bond yields a sizeable gain in energy, or that a rotation about another bond such as the amide  $C_1'-N_2'$  bond also yields a considerable gain in energy, but the two rotations together however yield a low energy structure, viz. the *EE*  $\rightarrow$  *EZ* transformation. One possible reason for this is the capability for hydrogen bonding in the *EZ* structure between H-4' and O-1' in (1)–(8). However ketimines (9) and (10) also exhibit the same behavior and all over ketimines (9) and (10) are not dissimilar to the azomethines (1)–(8) with the rotational energy barriers for the aforementioned rotations all falling within the ranges for (1)–(8) or being very close to them. The calculation of imine structures is neither trivial [40] nor is the recognition of cases of rapidly interconverting equilibria [40], but the results are in concert with the experimental observations regarding a strong bias towards an *E* configuration for the imine  $N_3=C_4$  double bond whilst the amide  $C_1'-N_2'$  bond is presumably a case of rapid interconversion given that only one set of signals was observed in solution.

### 3.3.2. Tautomerism

With the presence of two carbonyl groups and two NH groups, various tautomeric forms of compounds (1)–(10) can be antic-

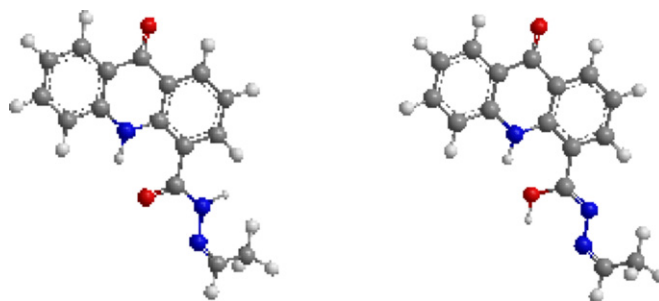


Fig. 7. The *H-10,H-2'* (left) and *H-10,H-1'* (right) tautomers of (7).

ipated, e.g. H-10 can be repositioned to the 9 position (i.e. a 9-hydroxy acridine structure) or even onto the amide carbonyl oxygen, whilst H-2' could be repositioned to the amide carbonyl oxygen (amide–iminol tautomerism) or onto C-4'. Further transpositions are also conceivable and the potential thus exists for the presence of numerous tautomers. Because of the intramolecular hydrogen bonding that exists between the amide carbonyl O-1' oxygen and H-10 proton in acridone [41], the 9-hydroxy acridine tautomers, though, were not considered likely to be energetically favored, whilst the  $H-10 \rightarrow H-1'$  and  $H-2' \rightarrow H-4'$  transpositions were omitted from examination. The N-10 atom of the acridinyl moiety in any event is well known [1,20–22,37,41–46] for its propensity to retain a proton, i.e. the *H-10* tautomer dominates the tautomeric equilibrium. In concert with this, the tautomeric equilibrium in acridone was found to favor the *H-10* tautomer by 13.16 kcal/mol (see [Supplementary material](#)). Furthermore, the  $NH_{10} \dots O_{1'}(=C)$  hydrogen bonding interaction in essence renders the distinction between the *H-10,H-2'* and *H-1',H-2'* tautomers moot. Thus, the amide–iminol tautomerism ( $H-2' \rightarrow H-1'$ ) and the  $H-10 \rightarrow H-9$  transpositions only were examined. That is, consideration was given to the four *H-10,H-2'*, *H-10,H-1'*, *H-9,H-2'* and *H-9,H-1'* tautomers (structures for the *H-10,H-2'* and *H-10,H-1'* tautomers presented in Fig. 7) to ascertain if a low content of the *H-10,H-1'* tautomer was present, either discretely or as part of a rapidly interconverting equilibrium (though bearing in mind that the accurate calculation of tautomers can be a challenge, especially with respect to geometry and the effect of solvent [47]). The calculated energies nevertheless showed that the *H-10,H-2'* tautomer is overwhelmingly favored with respect to the *H-10,H-1'* tautomer by at least 30 kcal/mol and by nearly 40 and 50 kcal/mol with respect to the *H-9,H-2'* and *H-9,H-1'* tautomers, respectively (see [Supplementary material](#)). Thus, these results substantiate the conclusions reached above in Section 3.2.1, viz. the  $^1H$ ,  $^{13}C$  and  $^{15}N$  NMR signals observed for the amide NH protons and nitrogens and the carbonyl carbons provide clear evidence based on their chemical shifts and correlations (Tables 2 and 4) that the tautomer *H-10,H-2'* is the only one present and other tautomers are not present, either as minor components in a slow exchange process or to a significant extent in the case of a rapidly interconverting equilibrium.

### 3.3.3. Hydrogen bonding

The intramolecular hydrogen bonding  $NH_{10} \dots O_{1'}(=C)$  present in (1)–(10) forms a six-membered, non-planar heterocycle:  $N_{10}-C_{4a}-C_4-C_1'-O_{1'} \dots H_{10}$  (see [Supplementary material](#) for intramolecular hydrogen bonding distances in molecules (1)–(10) calculated by DFT B3LYP/6-311+G(d,p) and AM1 methods). The dependence of the energy vs. the angle of rotation about the  $C_4-C_1'$  bond was evaluated by AM1 calculations (*vide supra*) whereby the energy was not found to be significantly increased for angle changes that would clearly disrupt the hydrogen bonding thereby implying that the intramolecular hydrogen bonding is weak and thus the stability of the six-membered ring is not considerable. An exam-

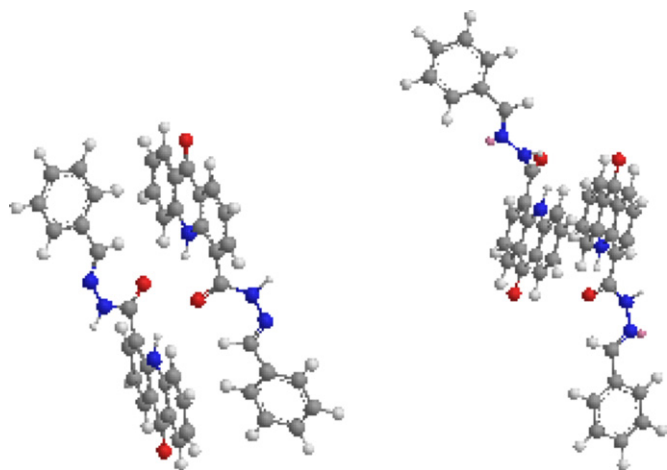


Fig. 8. The X (left) and Y (right) intermolecular hydrogen bonding models of (1).

ination of hydrogen bonding by AM1 calculations provided some interesting results: the formation of an intermolecular hydrogen bond  $\text{NH}_{10} \dots \text{O}_{1'}(=\text{C})$  (model X), i.e. between the  $\text{NH}_{10}$  hydrogen and the amide carbonyl O-1' oxygen, was found to be energetically preferable by 3.47 kcal/mol compared to the intermolecular hydrogen bond  $\text{NH}_{10} \dots \text{O}_9(=\text{C})$  (model Y), i.e. between the  $\text{NH}_{10}$  hydrogen and the acridone carbonyl O-9 oxygen (Fig. 8). Therefore the intermolecular hydrogen bonding evident by the IR examinations must be  $\text{NH}_{10} \dots \text{O}_{1'}(=\text{C})$ .

The calculated intermolecular distances between the hydrogen and oxygen (acridone) $\text{N}-\text{H} \dots \text{O}(\text{amidic})$  atomic pairs for model X are 2.257 and 2.276 Å and for model Y, 4.0621 and 4.1245 Å. The weak intramolecular hydrogen bonding and the preference for model X intermolecular hydrogen bonding suggest that two-centered hydrogen bonding on the carbonyl O-1' oxygen atom of the amide group atom may occur for compounds (1)–(10).

#### 4. Conclusions

Ten novel, potentially intercalating 4-acridonecarboxamide azomethines and ketimines have been prepared generally in high yields via the condensation reaction of 9-oxo-9,10-dihydroacridine-4-carboxylic acid hydrazide with various aldehydes and ketones in dry ethanol. The molecular structures of the synthesized compounds (1)–(10) were established and characterized spectroscopically by NMR ( $^1\text{H}$ ,  $^{13}\text{C}$ ,  $^{15}\text{N}$  and 2D experiments), UV–vis, IR and fluorescence methods and by quantum chemical calculations using DFT at the B3LYP/6-311 + G(d,p) level of theory and semiempirical ZINDO and AM1 methods.

It was observed that the  $^{13}\text{C}$  NMR chemical shifts of the C-4' carbons of the imine  $\text{C}_4=\text{N}_{3'}$  double bond in azomethines (1)–(8) are shielded in comparison to the corresponding carbon in ketimines (9) and (10), but the differences and variations within the series are due to changes in the polarizability of the imine  $\text{C}_4=\text{N}_{3'}$  double bond rather than due to direct inductive effects arising from the C-4' substituents. This is substantiated by a corresponding change observed for the N-3' nitrogens, but in reverse order to that observed for the C-4' carbons. Atomic charges obtained from the DFT calculations also confirmed the bond polarization. Other NMR parameters were within their expected ranges.

Intramolecular hydrogen bonds between the acridone  $\text{NH}_{10}$  hydrogen and the carbonyl O-1' oxygen of the amide group and intermolecular hydrogen bonds between the acridone  $\text{NH}_{10}$  hydrogen and the carbonyl O-1' oxygen of the amide group of another molecule were confirmed by FT-IR spectroscopy. Though the explicit identification of the intermolecular hydrogen bonds

could not be accomplished experimentally, quantum chemical calculations indicated that the energetically preferred hydrogen bonding was between the acridone H-10 hydrogen and the O-1' oxygen of the side chain amide group instead of the acridone O-9 carbonyl oxygen. Due to Fermi resonance consisting of four-level interactions, unperturbed values for the  $\nu(\text{N}_2-\text{H})$  stretch could not be extracted to provide an indication of the strength of the intramolecular hydrogen bonding. Quantum chemical calculations were also used to evaluate the conformational, tautomeric and configurational states of the molecules from which it was revealed that an *E* configuration for the imine  $\text{C}_4=\text{N}_{3'}$  double bond was energetically favored for the predominant *H*-10,*H*-2' tautomer.

The hypsochromic shifts observed in the UV–vis spectra upon a change of solvent from *m*-cresol to DMA, DMF or methanol were determined to result from excited state (de)stabilization by the solvent, i.e. the polar solvents could account for the hypsochromic shifts by excited state destabilization and/or the aromatic *m*-cresol could be responsible by inducing excited state stabilization. The fluorescence capabilities of compounds (1)–(10) were modest and only did the 2,6-dichloro derivative (5) compare favorably to the standard reference compound 9-isothiocyanatoacridine.

#### Acknowledgements

Financial support for this work by the Slovak Grant Agency VEGA (Grant No. 1/0476/08), the State NMR Program (grant no. 2003SP200280203), and Turun Yliopistosäätiö is gratefully acknowledged.

#### Appendix A. Supplementary data

Supplementary data associated with this article can be found, in the online version, at [doi:10.1016/j.saa.2009.02.016](https://doi.org/10.1016/j.saa.2009.02.016).

#### References

- [1] Z. Fröhlichová, J. Tomaščíková, J. Imrich, P. Kristian, I. Danihel, S. Böhm, D. Sabolová, M. Kožurková, K.D. Klika, *Heterocycles* 77 (2009) 1019.
- [2] A. Bouzyk, L. Jóźwiak, J. Błażejowski, *J. Mol. Struct.* 612 (2002) 29.
- [3] A. Iwan, B. Kaczmarczyk, H. Janeczek, D. Sek, S. Ostrowski, *Spectrochim. Acta, Part A* 66 (2007) 1030.
- [4] D. Sabolová, M. Kožurková, P. Kristian, I. Danihel, D. Podhradský, J. Imrich, *Int. J. Biol. Macromol.* 38 (2006) 94.
- [5] J.E. Sinsheimer, V. Jagodic, J. Polak, D.D. Hong, J.A. Burckhalter, *J. Pharm. Sci.* 64 (1975) 925.
- [6] M. Demeunynck, F. Charmantray, A. Martelli, *Curr. Pharm. Des.* 7 (2001) 1703.
- [7] V. Sourdon, S. Mazoyer, V. Pique, J.-P. Galay, *Molecules* 6 (2001) 677.
- [8] P. Kristian, *Chem. Pap. - Chem. Zvesti* 15 (1961) 164.
- [9] V. Sourdon, S. Mazoyer, V. Pique, J.P. Galy, *Molecules* 6 (2001) 673.
- [10] R.K. Harris, E.D. Becker, S.M. Cabral de Menezes, R. Goodfellow, P. Granger, *Pure Appl. Chem.* 73 (2001) 1795.
- [11] A.D. Becke, *J. Chem. Phys.* 98 (1993) 5648.
- [12] M.J. Frisch, G.W. Trucks, H.B. Schlegel, G.E. Scuseria, M.A. Robb, J.R. Cheeseman, J.A. Montgomery Jr., T. Vreven, K.N. Kudin, J.C. Burant, J.M. Millam, S.S. Iyengar, J. Tomasi, V. Barone, B. Mennucci, M. Cossi, G. Scalmani, N. Rega, A. Petersson, H. Nakatsuji, M. Hada, M. Ehara, K. Toyota, R. Fukuda, J. Hagesawa, M. Ishida, T. Nakajima, Y. Honda, O. Kitao, H. Nakai, M. Klene, X. Li, J.E. Knox, H.P. Hratchian, J.B. Cross, C. Adamo, J. Jaramillo, R. Gomperts, E. Stratmann, O. Yazyev, A.J. Austin, R. Cammi, C. Pomelli, J.W. Ochterski, P.Y. Ayala, K. Morokuma, G.A. Voth, P. Salvador, J.J. Dannenberg, V.G. Zakrzewski, S. Dapprich, A.D. Daniels, M.C. Strain, O. Farkas, D.K. Malick, A.D. Rabuck, K. Raghavachari, J.B. Foresman, J.V. Ortiz, Q. Cui, A.G. Baboul, S. Clifford, J. Cioslowski, B.B. Stefanov, G. Liu, A. Liashenko, P. Piskorz, I. Komaromi, R.L. Martin, D.J. Fox, T. Keith, M.A. Al-Laham, C.Y. Peng, A. Nanayakkara, M. Challacombe, P.M.W. Gill, B. Johnson, W. Chen, M.W. Wong, C. Gonzales, J.A. Pople, Gaussian03, Revision B.05, Gaussian, Inc., Pittsburgh, PA, 2003.
- [13] M.J.S. Dewar, E.G. Zoebisch, E.F. Healy, J.J.P. Stewart, *J. Am. Chem. Soc.* 107 (1985) 3902.
- [14] K. Wolinski, J.F. Hinton, P. Pulay, *J. Am. Chem. Soc.* 112 (1990) 8251.
- [15] J.B. Foresman, E. Frisch, *Exploring Chemistry with Electronic Structure Methods*, Second ed., Gaussian Inc., Pittsburgh, PA, USA, 1996.
- [16] L.K. Hanson, J. Fajer, M.A. Thompson, M.C. Zerner, *J. Am. Chem. Soc.* 109 (1987) 4728.
- [17] J.P. Kokko, J.H. Goldstein, *Spectrochim. Acta* 19 (1963) 1119.

- [18] G. Boyer, R.M. Claramunt, J. Elguero, M. Fathalla, C. Foces-Foces, C. Jaime, A.L. Llamas-Saiz, *J. Chem. Soc., Perkin Trans. 2* (1993) 757.
- [19] M.A. Alam, O. Ito, W. Adam, G.N. Grimm, C.R. Saha-Moeller, *Phys. Chem. Chem. Phys.* 1 (1999) 1851.
- [20] J. Tomaščíková, J. Imrich, I. Danihel, S. Böhm, P. Kristian, J. Písarčíková, M. Sabol, K.D. Klika, *Molecules* 13 (2008) 501.
- [21] K.D. Klika, E. Balentová, J. Bernát, J. Imrich, M. Vavrušová, E. Kleinpeter, K. Pihlaja, A. Koch, *J. Heterocycl. Chem.* 43 (2006) 633.
- [22] E. Balentová, J. Imrich, J. Bernát, L. Suchá, M. Vilková, N. Prónayová, P. Kristian, K. Pihlaja, K.D. Klika, *J. Heterocycl. Chem.* 43 (2006) 645.
- [23] J. Tomaščíková, J. Imrich, I. Danihel, S. Böhm, P. Kristian, *Collect. Czech. Chem. Commun.* 72 (2007) 347.
- [24] V. Vailikhit, W. Treesuwan, S. Hannongbua, *THEOCHEM* 806 (2007) 96.
- [25] O. Exner, S. Böhm, *Eur. J. Org. Chem.* (2007) 2870.
- [26] O. Hritzová, J. Černák, P. Šafař, Z. Fröhlichová, I. Csöreg, *J. Mol. Struct.* 743 (2005) 29.
- [27] K.V. Berezin, T.V. Krivokhizhina, V.V. Nechaev, *Opt. Spectrosc.* 100 (2006) (15 and references cited therein).
- [28] D. Hadži, J. Jan, *Spectrochim. Acta* 23A (1967) 571.
- [29] H. Wolff, H. Ludwig, *Ber. Bunsen Ges.* 70 (1966) 474.
- [30] H. Wolff, *J. Phys. Chem.* 52 (1972) 2800.
- [31] O. Hritzová, D. Koščík, *Collect. Czech. Chem. Commun.* 59 (1994) 951.
- [32] S. Bratos, *J. Chem. Phys.* 63 (1975) 3499.
- [33] S. Bratos, H. Ratajczak, *J. Chem. Phys.* 76 (1982) 77.
- [34] T. Miyazawa, *J. Mol. Spectrosc.* 4 (1960) 168.
- [35] R.A. Nyquist, H.A. Fouchea, G.A. Hoffman, D.L. Hasha, *Appl. Spectrosc.* 45 (1991) 860.
- [36] H.H. Jaffé, M. Orchin, *Theory and Application of Ultraviolet Spectroscopy*, J. Wiley & Sons, New York, 1966.
- [37] J. Bernát, E. Balentová, P. Kristian, J. Imrich, E. Sedlák, I. Danihel, S. Böhm, N. Prónayová, K. Pihlaja, K.D. Klika, *Collect. Czech. Chem. Commun.* 69 (2004) 833.
- [38] P. Kristian, J. Bernát, J. Imrich, E. Sedlák, J. Alföldi, M. Čornanič, *Heterocycles* 55 (2001) 279.
- [39] D. Mazagová, P. Kristian, G. Suchár, J. Imrich, M. Antalík, *Collect. Czech. Chem. Commun.* 59 (1994) 2632.
- [40] K.D. Klika, J. Imrich, I. Danihel, S. Böhm, P. Kristian, S. Hamul'aková, K. Pihlaja, A. Koch, E. Kleinpeter, *Magn. Reson. Chem.* 43 (2005) 380.
- [41] B. Adcock, Acridines, in: R.M. Acheson (Ed.), *Aminoacridines, from: The Chemistry of Heterocyclic Compounds*, A. Weissberger, E.C. Taylor (Eds.), J. Wiley & Sons, New York, 1973.
- [42] S. Hamul'aková, P. Kristian, D. Jun, K. Kuča, J. Imrich, I. Danihel, S. Böhm, K.D. Klika, *Heterocycles* 76 (2008) 1219.
- [43] K.D. Klika, E. Balentová, J. Bernát, J. Imrich, M. Vavrušová, K. Pihlaja, A. Koch, E. Kleinpeter, A. Kelling, U. Schilde, *ARKIVOC* (xvi) (2006) 93.
- [44] K.D. Klika, J. Imrich, M. Vilková, J. Bernát, K. Pihlaja, *J. Heterocycl. Chem.* 43 (2006) 739.
- [45] K.D. Klika, J. Bernát, J. Imrich, I. Chomča, R. Sillanpää, K. Pihlaja, *J. Org. Chem.* 66 (2001) 4416.
- [46] P. Kristian, E. Balentová, J. Bernát, J. Imrich, E. Sedlák, I. Danihel, S. Böhm, N. Prónayová, K.D. Klika, K. Pihlaja, J. Baranová, *Chem. Pap. - Chem. Zvesti* 58 (2004) 268.
- [47] J. Mäki, P. Tähtinen, L. Kronberg, K.D. Klika, *J. Phys. Org. Chem.* 18 (2005) 240.